Taylor & Francis
Taylor & Francis Group

Model reference tracking control of an aircraft: a robust adaptive approach

Ilker Tanyer[a], Enver Tatlicioglu[a] and Erkan Zergeroglu[b]

[a]Department of Electrical & Electronics Engineering, Izmir Institute of Technology, Izmir, Turkey; [b]Department of Computer Engineering, Gebze Technical University, Kocaeli, Turkey

ABSTRACT

This work presents the design and the corresponding analysis of a nonlinear robust adaptive controller for model reference tracking of an aircraft that has parametric uncertainties in its system matrices and additive state- and/or time-dependent nonlinear disturbance-like terms in its dynamics. Specifically, robust integral of the sign of the error feedback term and an adaptive term is fused with a proportional integral controller. Lyapunov-based stability analysis techniques are utilised to prove global asymptotic convergence of the output tracking error. Extensive numerical simulations are presented to illustrate the performance of the proposed robust adaptive controller.

1. Introduction

Amongst the control techniques applied on aerial vehicles, adaptive methods are very common (Dydek, Annaswamy, & Lavretsky, 2010; How, Frazzoli, & Chowdhary, 2012; Stevens & Lewis, 2003). In adaptive methods, upon satisfaction of a linear parametrisation property, an update rule is designed to compensate for the lack of accurate knowledge of constant or slowly-varying model parameters (Ioannou & Sun, 1995). Doman and Ngo (2002) designed a dynamic inversion-based adaptive controller for attitude tracking of a spacecraft. Tandale and Valasek (2005) proposed an adaptive dynamic inversion-based switching control methodology to compensate for parametric uncertainties. Chen, Li, Jiang, and Sun (2006) developed an adaptive dynamic inversion controller for a flexible spacecraft. To compensate for parametric uncertainties, Lavretsky and Hovakimyan (2005) designed a direct model reference adaptive controller fused with a dynamic inversion controller. While adaptive methods can successfully compensate for parametric uncertainties, their performance is not satisfactory when the model parameters vary fastly and/or there are unstructured uncertainties. Thus, some past research was devoted to robustifying the adaptive methods to compensate for both parametric and unstructured uncertainties. Some part of the past research focused on utilising neural networks in conjunction with adaptive controllers (Calise & Rysdyk, 1998; Liu et al., 2004). Liu et al. (2004) used dynamic inversion method in conjunction with a nonlinear model reference adaptive controller based on neural networks. Calise and Rysdyk (1998) proposed an adaptive dynamic inversion-based controller which was a combination of adaptive feedforward neural networks with feedback linearisation. Some line of past research has focused on utilising robust components in conjunction with adaptive controllers (MacKunis, Patre, Kaiser, & Dixon, 2010; Mondal & Mahanta, 2012; Wang, Li, & Wang, 2011). Mondal and Mahanta (2012) designed an adaptive second-order sliding-mode controller for stabilising and trajectory tracking of a twin rotor

system. To compensate for modelling errors and external disturbances, Wang et al. (2011) designed an adaptive dynamic inversion-based controller for a miniature unmanned aerial vehicle (UAV). MacKunis et al. (2010) proposed two controllers for UAVs where one of them was a robust adaptive controller. The authors obtained exponential output tracking when aircraft dynamics were uncertain and the aircraft was considered to be subject to additive disturbances. The main drawback of the proposed controller was that the sign of the time derivative of the output was required (i.e. sign of the acceleration measurements were needed).

In this paper, model reference tracking control of an aircraft is considered. Only the output of the aircraft is considered to be available for the control design (i.e. neither the acceleration information nor its sign are not available). The dynamic model of the aircraft is considered to be uncertain (i.e. the state and the input matrices are uncertain) and also subject to uncertain additive disturbances. Due to the uncertainties of the system matrices, the input gain matrix is uncertain. When constructing the error system, a matrix decomposition is utilised to cope with possibly sign indefinite and not necessarily symmetric input gain matrix. When the system is subject to unstructured uncertainties in addition to parametric uncertainties, robust adaptive control is usually the preferred method. Robust adaptive control was applied to surface vessels (Annamalai, Sutton, Yang, Culverhouse, & Sharma, 2015; Do, 2016), robot manipulators (Carrasco-Elizalde & Goldsmith, 2015; Tatlicioglu, 2010; Yu & Fei, 2014; Yu, Fei, Sun, Huang, & Yang, 2014, 2015), mechatronic systems (Bidikli, Tatlicioglu, & Zergeroglu, 2015; Fei & Zhou, 2012), electrical systems (Khooban, Niknam, Blaabjerg, Davari, & Dragicevic, 2016; Tan, Su, Zhao, & Tan, 2015), multi-input multi-output nonlinear systems (Bayrak, Tatlicioglu, Bidikli, & Zergeroglu, 2013; Hussain, Annaswamy, & Lavretsky, 2016; Jafari & Ioannou, 2016; Yildiz & Annaswamy, 2015; Yu, Fei, & Yang, 2015), and aerial vehicles (Wise, Lavretsky, Gadient, & Ioannou, 2015; Xu, 2015; Zhao, Xian, Zhang,

& Zhang, 2015; Zou, Wang, Zou, & Zong, 2015; Zou, 2016). In the controller design, an adaptive term fused with integral of the sign of the tracking error feedback is utilised. The proposed controller ensures global asymptotic stability of the tracking error via the use of Lyapunov-based design and analysis techniques. Extensive numerical studies are presented to demonstrate the performance of the robust adaptive controller.

2. Aircraft model

In this paper, to represent the equation of motion of an aircraft, the following nonlinear state-space model is considered (Stevens & Lewis, 2003):

$$\dot{x} = Ax + f(x, t) + Bu, \quad y = Cx, \tag{1}$$

where $x(t) \in \mathbb{R}^n$ is the state vector, $A \in \mathbb{R}^{n \times n}$ is the constant state matrix, $f(x, t) \in \mathbb{R}^n$ is a state- and time-dependent disturbance-like term which includes modelling effects such as gravity, inertial coupling and nonlinear gust, $B \in \mathbb{R}^{n \times m}$ is the constant input matrix, $u(t) \in \mathbb{R}^m$ denotes the control input, $C \in \mathbb{R}^{m \times n}$ is the output matrix, and $y(t) \in \mathbb{R}^m$ is the output.

The aircraft model considered in this work has more states than the outputs (i.e. $n > m$). In the above model, as a direct consequence of the varying nature of aircraft dynamics due to operating conditions, A, B and f are uncertain, and only C is considered to be known accurately. The nonlinear disturbance-like term $f(x, t)$ is considered to be equal to the sum of state-dependent uncertainties, denoted by $f_1(x) \in \mathbb{R}^n$, and time-dependent uncertainties, denoted by $f_2(t) \in \mathbb{R}^n$ (see MacKunis, 2009 for the precedence of this type of segregation). The time-dependent uncertainty vector $f_2(t)$ is considered to be continuously differentiable and bounded up to its first-order time derivative, while the state-dependent uncertainty vector $f_1(x)$ depends on the state vector $x(t)$ via trigonometric and/or bounded arguments only and thus $f_1(x)$ and $\partial f_1(x)/\partial x$ are bounded for all $x(t)$. As discussed by Arapostathis, George, and Ghosh (2001), when f satisfies the above in addition to (A, B) being a controllable pair, then the nonlinear state-space model of the aircraft in (1) is controllable.

3. Control design

The main objective is to design a control law to ensure that the output of the aircraft $y(t)$ tracks the output of a reference aircraft model. The control problem is complicated by the unavailability of full-state feedback and by A, B and f being uncertain. The secondary control objective is to guarantee that all signals remain bounded under the closed-loop operation.

The reference model has the following form:

$$\dot{x}_m = A_m x_m + B_m u_m, \quad y_m = C x_m, \tag{2}$$

where $x_m(t) \in \mathbb{R}^n$ is the reference state vector, $A_m \in \mathbb{R}^{n \times n}$ is the reference state matrix, $B_m \in \mathbb{R}^{n \times m}$ is the reference input matrix, $u_m(t) \in \mathbb{R}^m$ is the reference input, C is the same output matrix introduced in (1), and $y_m(t) \in \mathbb{R}^m$ is the reference output. To ensure the stability of the reference model, the reference state matrix A_m is required to be Hurwitz in addition to the reference input $u_m(t)$ and its time derivative being bounded functions of time. Therefore, $x_m(t)$ and its first two time derivatives,

and, thus, $y_m(t)$ and its first two time derivatives are bounded functions of time.

The output tracking error, denoted by $e(t) \in \mathbb{R}^m$, is defined as

$$e \triangleq y - y_m. \tag{3}$$

To have a stability analysis with only first-order time derivatives of the error vectors, an auxiliary error vector, denoted by $r(t) \in \mathbb{R}^m$, is defined as (Dawson, Hu, & Burg, 1998; Dixon, Behal, Dawson, & Nagarkatti, 2003)

$$r \triangleq \dot{e} + \Lambda e, \tag{4}$$

where $\Lambda \in \mathbb{R}^{m \times m}$ is a constant, positive-definite, diagonal control gain matrix.

Taking the time derivative of (4) along with (1)–(3) yields

$$\dot{r} = CA\dot{x} + CB\dot{u} + C\dot{f} - CA_m\dot{x}_m - CB_m\dot{u}_m + \Lambda\dot{e} \tag{5}$$

in which the input gain matrix CB is uncertain since B is uncertain. To deal with this, the SDU decomposition in Costa, Hsu, Imai, and Kokotović (2003) is applied to obtain $CB = SDU$, where $S \in \mathbb{R}^{m \times m}$ is a symmetric, positive-definite matrix, $D \in \mathbb{R}^{m \times m}$ is a diagonal matrix with entries ± 1, and $U \in \mathbb{R}^{m \times m}$ is a unity upper triangular matrix. The details of the SDU decomposition can be found in Tao (2003). Since S is symmetric and positive-definite, its inverse $M \triangleq S^{-1} \in \mathbb{R}^{m \times m}$ is also symmetric and positive-definite. Pre-multiplying (5) with M yields

$$M\dot{r} = -e + DU\dot{u} + N, \tag{6}$$

where $N(x, \dot{x}, t) \in \mathbb{R}^m$ is defined as

$$N \triangleq M[CA\dot{x} + C\dot{f} - CA_m\dot{x}_m - CB_m\dot{u}_m + \Lambda\dot{e}] + e. \tag{7}$$

The above auxiliary term is now partitioned as

$$N = N_{LP} + N_d + \widetilde{N}, \tag{8}$$

where $N_{LP}(t)$, $N_d(t)$, $\widetilde{N}(x, \dot{x}, e, r) \in \mathbb{R}^m$. In the above partitioning, first, the terms that can be written as a multiplication of measurable and known quantities with uncertain constant model parameters were grouped into $N_{LP}(t) \triangleq MCA\dot{x}_m - MCA_m\dot{x}_m - MCB_m\dot{u}_m$; next, the remaining terms were grouped into $N_d(t) \triangleq MC\dot{f}_2 + MC\frac{\partial f_1}{\partial x}\dot{x}_m$ which includes terms that are bounded by constants, or into $\widetilde{N}(t) \triangleq MCA(\dot{x} - \dot{x}_m) + MC\frac{\partial f_1}{\partial x}(\dot{x} - \dot{x}_m) + M\Lambda r - M\Lambda^2 e + e$ which includes terms that are bounded by functions of error signals. By utilising the boundedness of the modelling uncertainty vector f and the reference model signals, it can be shown that $N_d(t)$ is a bounded function of time in the sense that $|N_{d,i}| \leq \zeta_{N_{d,i}} \ \forall t$ with $\zeta_{N_{d,i}} \in \mathbb{R}$ being known positive bounding constants (or alternatively, $\|N_d(t)\| \leq \zeta_{N_d} \ \forall t$ where $\zeta_{N_d} \in \mathbb{R}$ is a known positive bounding constant). The entries of the auxiliary vector $\widetilde{N}(t)$ can be upper bounded as $|\widetilde{N}_i| \leq \rho_i \|z(t)\|$ with $\rho_i \in \mathbb{R}$ being known positive bounding constants (or alternatively $\|\widetilde{N}(t)\| \leq \rho \|z(t)\|$ where $\rho \in \mathbb{R}$ is a known positive bounding constant).
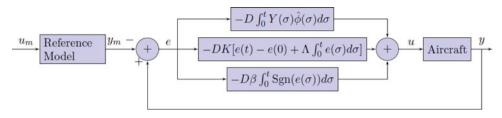
Figure 1. The block diagram of the closed-loop system.

It is important to highlight that the linear parametrisation is obtained from a different structure than most of the past gradient-based adaptive works. Specifically, the linear parametrisation has the form

$$Y\phi = N_{LP} - D(U - I_m)DY\hat{\phi}, \tag{9}$$

where $Y(t) \in \mathbb{R}^{m \times p}$ denotes the regression matrix which is composed of reference signal, its time derivatives, and other known quantities and $\phi \in \mathbb{R}^p$ is the unknown parameter vector with $\hat{\phi}(t) \in \mathbb{R}^p$ being its yet-to-be-designed estimate. The main motivation of the novel definition in (9) is due to the pre-multiplication of the time derivative of the control input and thus its adaptive component with DU. The consequence of this is a term that has the form $DUDY\hat{\phi}$ where U is also uncertain. Rewriting $DUDY\hat{\phi}$ as sum of $Y\hat{\phi}$ and $D(U - I_m)DY\hat{\phi}$ helps in achieving the adaptation in the sense that $Y\hat{\phi}$ is the adaptation term and $D(U - I_m)DY\hat{\phi}$ can be written as a multiplication of a known regression matrix that depends on known and available terms $D, Y, \hat{\phi}$ with an uncertain constant vector that is obtained from the entries of U. As a result of this segregation, $D(U - I_m)DY\hat{\phi}$ can be written as part of (9). Since U is unity upper triangular, then $U - I_m$ is strictly upper triangular so there is no algebraic loop in finding $Y(t)$ from (9).

The control input is designed as

$$u = -DK\left[e(t) - e(0) + \Lambda \int_0^t e(\sigma)d\sigma\right]$$
$$- D\Pi - D\int_0^t Y(\sigma)\hat{\phi}(\sigma)d\sigma, \tag{10}$$

where $\Pi(t) \in \mathbb{R}^m$ is an auxiliary filter vector updated according to

$$\dot{\Pi}(t) = \beta\, \mathrm{Sgn}(e(t)) \text{ with } \Pi(0) = 0_{m \times 1} \tag{11}$$

and $\beta \in \mathbb{R}^{m \times m}$ is a constant, positive-definite, diagonal, control gain matrix, $\mathrm{Sgn}(\cdot)$ denotes the vector sign function, $K \in \mathbb{R}^{m \times m}$ is a constant, positive-definite, diagonal, control gain matrix and is chosen as

$$K = I_m + k_g I_m + \mathrm{diag}\{k_{d,1}, k_{d,2}, \ldots, k_{d,m-1}, 0\} \tag{12}$$

with $k_g, k_{d,1}, \ldots, k_{d,m-1} \in \mathbb{R}$ being positive gains, and the adaptive update rule is designed as

$$\hat{\phi} = \mathrm{Proj}\left(\Gamma(Y^T e - \int_0^t \frac{dY^T(\sigma)}{d\sigma}e(\sigma)d\sigma\right.$$
$$\left. + \int_0^t Y^T(\sigma)\Lambda e(\sigma)d\sigma)\right), \tag{13}$$

where $\mathrm{Proj}(.)$ is the projection operator that ensures the boundedness of the parameter estimate vector and its time derivative (Krstic, Kanellakopoulos, & Kokotovic, 1995). The control input in (10) and (11) is a nonlinear proportional integral controller fused with an adaptive component to compensate for parametric uncertainties and with integral of sign of error feedback terms for unstructured uncertainty compensation. The block diagram of the closed-loop system is presented in Figure 1.

After substituting the time derivative of the control input in (10) into (6), the closed-loop error dynamics for $r(t)$ is obtained as

$$M\dot{r} = \widetilde{N} + N_d - e - [\Phi^T, 0]^T$$
$$- Kr - DUD\beta\mathrm{Sgn}(e) + Y\widetilde{\phi}, \tag{14}$$

where (4), (8), (9) and (11) were utilised, $\widetilde{\phi}(t) \triangleq \phi - \hat{\phi} \in \mathbb{R}^p$ is the parameter estimation error, and $\Phi(r) \in \mathbb{R}^{(m-1) \times 1}$ is obtained from $D(U - I_m)DKr = [\Phi^T, 0]^T$. The entries of $\Phi(r)$ denoted by $\Phi_i(r)$ can be upper bounded as $|\Phi_i(r)| \le \zeta_{\Phi_i}\|z\|$ for some positive bounding constants ζ_{Φ_i}. The term $DUD\beta\mathrm{Sgn}(e)$ can be rewritten as $DUD\beta\mathrm{Sgn}(e) = [\Psi^T, 0]^T + \beta\mathrm{Sgn}(e)$, where the entries of $\Psi(t) \in \mathbb{R}^{(m-1) \times 1}$ can be upper bounded as $|\Psi_i| \le \zeta_{\Psi_i}$ where $\zeta_{\Psi_i} \in \mathbb{R}$ are positive bounding constants.

4. Stability analysis

Theorem 4.1: *The controller in* (10) *and* (11) *with the adaptive update rule in* (13) *ensures global asymptotic output tracking in the sense that* $\|e(t)\| \to 0$ *as* $t \to \infty$ *when the entries of the control gain matrices K and* β *are selected by using the following procedure:*

(1) β_m *is selected according to*

$$\beta_m \ge \zeta_{N_{d,m}}\left(1 + \frac{\kappa_2}{\Lambda_m}\right), \tag{15}$$

where $\kappa_2 \in \mathbb{R}$ is some positive bounding constant, $\zeta_{N_{d,m}}$ is defined in (8), and the subscript $i = 1, \ldots, m$ denotes the i-th element of the vector or the diagonal matrix,

(2) β_i for $i = m - 1$ to $i = 1$ are selected according to

$$\beta_i \geq \left(\zeta_{N_{d,i}} + \sum_{j=i+1}^{m} \zeta_{\Psi_j} \beta_j \right) \left(1 + \frac{\kappa_2}{\Lambda_i} \right), \qquad (16)$$

where $\zeta_{N_{d,i}}$ is defined in (8) and ζ_{Ψ_j} is introduced in (14),

(3) k_g is chosen to decrease the constant $\frac{\rho^2}{4k_g}$, where ρ is defined in (8),

(4) $k_{d,\,i}, i = 1, \ldots, (m - 1)$ are chosen to decrease the constant $\sum_{i=1}^{m-1} \frac{\zeta_{\Phi_i}^2}{4k_{d,i}}$, where ζ_{Φ_i} is defined in (14).

Proof: First, the proof of the boundedness of all the signals under the closed-loop operation will be demonstrated. Let $V_b(z) \in \mathbb{R}$ be a Lyapunov function defined as

$$V_b \triangleq \frac{1}{2} e^T e + \frac{1}{2} r^T M r, \qquad (17)$$

which can be upper and lower bounded as

$$\frac{1}{2} \min\{1, M_{\min}\} \|z\|^2 \leq V_b(z) \leq \frac{1}{2} \max\{1, M_{\max}\} \|z\|^2, \qquad (18)$$

where $M_{\min}$ and $M_{\max}$ denote minimum and maximum eigenvalues of M, respectively. After utilising the symmetry of M, time derivative of the Lyapunov function can be written as

$$\dot{V}_b = e^T \dot{e} + r^T M \dot{r} \qquad (19)$$

to which substituting (4) and (12), and then canceling common terms with opposite signs gives

$$\dot{V}_b = -e^T \Lambda e + r^T N_d + r^T \widetilde{N} - r^T DUD\beta \mathrm{Sgn}(e)$$
$$- r^T \begin{bmatrix} \Phi \\ 0 \end{bmatrix} - r^T r - k_g r^T r - \sum_{i=1}^{m-1} k_{d,i} r_i^2 + r^T Y \widetilde{\phi}. \qquad (20)$$

Substituting the upper bounds of the entries of N_d, $\widetilde{N}$ and Φ yields in

$$\dot{V}_b \leq -e^T \Lambda e + \sum_{i=1}^{m} \zeta_{N_{d,i}} |r_i| + \sum_{i=1}^{m} \rho_i |r_i| \|z\| + \zeta_1 \|r\|$$
$$+ \sum_{i=1}^{m-1} \zeta_{\Phi_i} |r_i| \|z\| - \|r\|^2 - k_g \|r\|^2 - \sum_{i=1}^{m-1} k_{d,i} r_i^2, \qquad (21)$$

where the upper bound $|r^T DUD\beta \mathrm{Sgn}(e)| + |r^T Y \widetilde{\phi}| \leq \zeta_1 \|r\|$ with $\zeta_1 \in \mathbb{R}$ being a positive bounding constant was also utilised. After utilising following manipulations

$$\zeta_1 \|r\| + \sum_{i=1}^{m} \zeta_{N_{d,i}} |r_i| \leq \frac{1}{2\delta} \|r\|^2 + \delta \left(\zeta_1^2 + \sum_{i=1}^{m} \zeta_{N_{d,i}}^2 \right) \qquad (22)$$

$$\rho_i |r_i| \|z\| - k_g r_i^2 \leq \frac{\rho_i^2}{4k_g} \|z\|^2 \qquad (23)$$

$$\zeta_{\Phi_i} |r_i| \|z\| - k_{d,i} r_i^2 \leq \frac{\zeta_{\Phi_i}^2}{4k_{d,i}} \|z\|^2 \qquad (24)$$

$\forall i = 1, \ldots, (m - 1)$, where $\delta \in \mathbb{R}$ is a positive damping constant, the right-hand side of (21) can be upper bounded as

$$\dot{V}_b \leq - \left[\min\left\{ \Lambda_{\min}, \left(1 - \frac{1}{2\delta} \right) \right\} - \sum_{i=1}^{m} \frac{\rho_i^2}{4k_g} - \sum_{i=1}^{m-1} \frac{\zeta_{\Phi_i}^2}{4k_{d,i}} \right] \|z\|^2$$
$$+ \delta \left(\zeta_1^2 + \sum_{i=1}^{m} \zeta_{N_{d,i}}^2 \right), \qquad (25)$$

where $\Lambda_{\min}$ denotes the minimum eigenvalue of Λ. When the gains Λ, k_g, $k_{d,1}$,..., $k_{d,m-1}$ are selected sufficiently high, from (25), the following expression can be reached:

$$\dot{V}_b \leq -c_1 V_b + c_2, \qquad (26)$$

where (18) was utilised and c_1 and c_2 are positive bounding constants defined as

$$c_1 \triangleq \frac{2}{\max\{1, M_{\max}\}} \left[\min\left\{ \Lambda_{\min}, \left(1 - \frac{1}{2\delta} \right) \right\} \right.$$
$$\left. - \sum_{i=1}^{m} \frac{\rho_i^2}{4k_g} - \sum_{i=1}^{m-1} \frac{\zeta_{\Phi_i}^2}{4k_{d,i}} \right] \qquad (27)$$

$$c_2 \triangleq \delta \left(\zeta_1^2 + \sum_{i=1}^{m} \zeta_{N_{d,i}}^2 \right). \qquad (28)$$

From (26), it is clear that $V_b(t) \in L_\infty$, and, thus, $e(t), r(t) \in L_\infty$. From (4), it can be proven that $\dot{e}(t) \in L_\infty$. By using (3) and its time derivative, along with the boundedness of reference model signals, it can be proven that $y(t), \dot{y}(t), x(t), \dot{x}(t) \in \mathcal{L}_\infty$. The above boundedness statements along with the properties of $f(x, t)$ can be utilised with (1) to prove that $u(t) \in \mathcal{L}_\infty$. From the time derivative of the control input in (10), it is clear that $\dot{u}(t) \in \mathcal{L}_\infty$. After utilising the above boundedness statements along with the properties of $f(x, t)$ and boundedness of the reference model signals along with (5), it can be proven that $\dot{r}(t) \in \mathcal{L}_\infty$. Standard signal chasing algorithms can be used to prove that all the remaining signals are bounded.

The following proposition, which makes use of the boundedness of the tracking error and its time derivative is the second step of the proof of the theorem. Specifically, provided that the entries of $e(t)$ and $\dot{e}(t)$ are bounded, the following expression can be obtained:

$$\int_{t_0}^{t} |\dot{e}_i(\sigma)| d\sigma \leq \kappa_1 + |e_i(t)| + \kappa_2 \int_{t_0}^{t} |e_i(\sigma)| d\sigma, \qquad (29)$$

where κ_1, $\kappa_2 \in \mathbb{R}$ are some positive bounding constants. The proof of this proposition is available in Stepanyan and Kurdila (2009) and Tanyer, Tatlicioglu, and Zergeroglu (2014).

Now, an auxiliary Lyapunov-like function will be introduced. This function will later be utilised in analysing the stability of the output tracking error. Specifically, let $L(t) \in \mathbb{R}$ be an auxiliary function defined as

$$L \triangleq r^T [N_d - DUD\beta \text{Sgn}(e)]. \quad (30)$$

If the entries of β are selected to satisfy (15) and (16), then the auxiliary function $P(t) \in \mathbb{R}$, defined as

$$P \triangleq \zeta_b - \int_0^t L(\sigma)\,d\sigma, \quad (31)$$

is non-negative, where $\zeta_b \in \mathbb{R}$ is a positive bounding constant. The proof of non-negativeness of P can be found in Bidikli, Tatlicioglu, Zergeroglu, and Bayrak (2016) and Tanyer (2015). The auxiliary function $P(t)$ will later be utilised as part of the Lyapunov function and will cancel out the uncertain vector $N_d(t)$.

Now, the asymptotic stability of the output tracking error is presented. Let $V_s(w) \in \mathbb{R}$ be a Lyapunov function defined as

$$V_s \triangleq V_b + \frac{1}{2}\widetilde{\phi}^T \Gamma^{-1} \widetilde{\phi} + P, \quad (32)$$

where $w(t) \triangleq \begin{bmatrix} e^T & r^T & \widetilde{\phi}^T & \sqrt{P} \end{bmatrix}^T \in \mathbb{R}^{(2m+p+1)\times 1}$ and $V_b(z)$ is defined in (17). Notice that, non-negativeness of $V_s(w)$ is ensured via the non-negativeness of $P(t)$. The Lyapunov function in (32) can be upper and lower bounded as

$$\frac{1}{2}\min\left\{1, M_{\min}, \frac{1}{\Gamma_{\max}}\right\}\|w\|^2 \leq V_s(w)$$
$$\leq \max\left\{\frac{1}{2}M_{\max}, 1, \frac{1}{2\Gamma_{\min}}\right\}\|w\|^2, \quad (33)$$

where $\Gamma_{\max}$ and $\Gamma_{\min}$ denote maximum and minimum eigenvalues of Γ, respectively.

Taking the time derivative of (32), substituting (4) and (14), and time derivatives of (13) and (31), results in

$$\dot{V}_s \leq e^T(r - \Lambda e) + r^T[N_d + \widetilde{N} - e - [\Phi^T, 0]^T$$
$$- r - k_g r - \text{diag}\{k_{d,1}, k_{d,2}, \ldots, k_{d,m-1}, 0\}r$$
$$- DUD\beta \text{Sgn}(e) + Y\widetilde{\phi}] - \widetilde{\phi}^T Y^T r$$
$$- r^T[N_d - DUD\beta \text{Sgn}(e)], \quad (34)$$

where $-\widetilde{\phi}^T \Gamma^{-1} \dot{\widetilde{\phi}} \leq -\widetilde{\phi}^T Y^T r$, which is a property of the projection operator (Krstic et al., 1995), was utilised. After canceling the same terms with opposite signs and then making use of the nonlinear damping argument, the right-hand side of (34) can be upper bounded as

$$\dot{V}_s \leq -\left[\min\{\Lambda_{\min}, 1\} - \frac{\rho^2}{4k_g} - \sum_{i=1}^{m-1} \frac{\zeta_{\Phi_i}^2}{4k_{d,i}}\right]\|z\|^2, \quad (35)$$

where $\Lambda_{\min}$ denotes the minimum eigenvalue of Λ. Provided that the control gains Λ, k_g, $k_{d,1}, \ldots, k_{d,m-1}$ are selected sufficiently high, the following expression can be obtained:

$$\dot{V}_s \leq -c_3\|z\|^2, \quad (36)$$

where c_3 is some positive bounding constant. From (32) and (36), it is clear that $V_s(w)$ is non-increasing and bounded. After integrating (36) in time from t_0 to $+\infty$, it is easy to see that $z(t) \in \mathcal{L}_2$. Since $z(t) \in \mathcal{L}_2 \cap \mathcal{L}_\infty$ and $\dot{z}(t) \in \mathcal{L}_\infty$, from Barbalat's Lemma in Khalil (2002), $\|z(t)\| \to 0$ as $t \to \infty$, thus meeting the tracking control objective. Since no restrictions with respect to the initial conditions of the error signals were imposed on the control gains, the result is global. ∎

The stability analysis requires the control gains β and K to be chosen to satisfy the procedure in Theorem 4.1. In choosing these control gains, the self-adjusting method in Bidikli, Tatlicioglu, Bayrak, and Zergeroglu (2013) and Bidikli, Tatlicioglu, and Zergeroglu (2014) which was designed for similar type of robust controllers can be used. The entries of gain matrices β and K are self-tuned according to

$$\beta_i(t) = \beta_{ci} + |e_i(t)| - |e_i(0)| + \Lambda_i \int_0^t |e_i(\sigma)|\,d\sigma \quad (37)$$

$$K_i(t) = k_{ci} + \frac{1}{2}e_i^2(t) - \frac{1}{2}e_i^2(0) + \Lambda_i \int_0^t e_i^2(\sigma)\,d\sigma \quad (38)$$

for $i = 1, \ldots, m$, where $\beta_{ci}, k_{ci} \in \mathbb{R}$ are positive constant parts of the time-varying gains that can be chosen freely.

5. Simulation results

To demonstrate the performance of the proposed adaptive controller, numerical simulations were conducted on the model of Osprey fixed-wing aerial vehicle in MacKunis et al. (2010) and MacKunis (2009), which is based on experimentally determined data at a cruising velocity of 25 m/s and at an altitude of 60 m. Provided the standard assumption that the longitudinal and lateral subsystems of the aircraft are decoupled, the model of Osprey aircraft testbed can be represented as in (1). The state vector $x(t) = \begin{bmatrix} x_{lon}^T, x_{lat}^T \end{bmatrix}^T \in \mathbb{R}^8$ where $x_{lon}(t), x_{lat}(t) \in \mathbb{R}^4$ denote longitudinal and lateral state vectors and are defined as $x_{lon} = [v, \alpha, q, \theta]^T$ and $x_{lat} = [\gamma, p, \mu, \phi]^T$, where $v(t), \alpha(t), q(t), \theta(t), \gamma(t), p(t), \mu(t)$ and $\phi(t)$ are velocity, angle of attack, pitch rate, pitch angle, side slip angle, roll rate, yaw rate and bank angle, respectively. The system matrices $A \in \mathbb{R}^{8\times 8}$, $B \in \mathbb{R}^{8\times 4}$, $C \in \mathbb{R}^{4\times 8}$ are given as

$$A = \begin{bmatrix} A_{lon} & 0_{4\times 4} \\ 0_{4\times 4} & A_{lat} \end{bmatrix} \quad B = \begin{bmatrix} B_{lon} & 0_{4\times 2} \\ 0_{4\times 2} & B_{lat} \end{bmatrix} \quad C = \begin{bmatrix} C_{lon} & 0_{2\times 4} \\ 0_{2\times 4} & C_{lat} \end{bmatrix}, \quad (39)$$

where $A_{lon}, A_{lat} \in \mathbb{R}^{4\times 4}$, $B_{lon}, B_{lat} \in \mathbb{R}^{4\times 2}$, $C_{lon}, C_{lat} \in \mathbb{R}^{2\times 4}$ are system matrices for longitudinal and lateral subsystems which have the form

$$A_{lon} = \begin{bmatrix} -0.15 & 11.08 & 0.08 & 0 \\ -0.03 & -7.17 & 0.83 & 0 \\ 0 & -37.35 & -9.96 & 0 \\ 0 & 0 & 1 & 0 \end{bmatrix}$$

$$A_{lat} = \begin{bmatrix} -0.69 & -0.03 & -0.99 & 0 \\ -3.13 & -12.92 & 1.1 & 0 \\ 17.03 & -0.10 & -0.97 & 0 \\ 0 & 1 & -0.03 & 0 \end{bmatrix}$$

$$B_{lon} = \begin{bmatrix} 3 \times 10^{-3} & 0.06 \\ 10^{-5} & 10^{-4} \\ 0.98 & 0 \\ 0 & 0 \end{bmatrix} \quad B_{lat} = \begin{bmatrix} 0 & 0 \\ 1.5 & -0.02 \\ -0.09 & 0.17 \\ 0 & 0 \end{bmatrix}$$

$$C_{lon} = \begin{bmatrix} 0 & 0 & 1 & 0 \\ 1 & 0 & 0 & 0 \end{bmatrix} \quad C_{lat} = \begin{bmatrix} 0 & 1 & 0 & 0 \\ 0 & 0 & 1 & 0 \end{bmatrix}. \quad (40)$$

The disturbance-like vector $f(x, t) \triangleq [f_{lon}(x, t)^T, f_{lat}(x, t)^T]^T$ with $f_{lon}(x, t)$, $f_{lat}(x, t) \in \mathbb{R}^4$ being modelled as

$$f_{lon} \triangleq \begin{bmatrix} -9.81 \sin \theta \\ 0 \\ 0 \\ 0 \end{bmatrix} + g(x), \quad f_{lat} \triangleq \begin{bmatrix} 0.39 \sin \phi \\ 0 \\ 0 \\ 0 \end{bmatrix}, \quad (41)$$

where $g(x) \in \mathbb{R}^4$ has the following form:

$$g \triangleq \frac{1}{V_0} \frac{U_{ds}}{2} \left[1 - \cos \left(\frac{\pi d_g}{H} \right) \right] \begin{bmatrix} -11.1 \\ 7.2 \\ 37.4 \\ 0 \end{bmatrix}, \quad (42)$$

where H denotes the distance along the airplane's flight path for the gust to reach its peak velocity, V_0 is the forward velocity of the aircraft when it enters the gust, $d_g = \int_{t_1}^{t_2} V(t) dt$ represents the distance penetrated into the gust and U_{ds} is the design gust velocity as specified in Federal Aviation Administration (2002). Parameter values were chosen as $U_{ds} = 10.12$ m/s, $H = 15.24$ m and $V_0 = 25$ m/s (MacKunis et al., 2010). To demonstrate robustness to noise, additive white Gaussian noise with signal-to-noise ratio of 20 dB was added to the velocity measurements.

The following matrices were utilised for the reference model

$$A_{lonm} = \begin{bmatrix} 0.6 & -1.1 & 0 & 0 \\ 2 & -2.2 & 0 & 0 \\ 0 & 0 & -4 & -600 \\ 0 & 0 & 0.1 & -10 \end{bmatrix}$$

$$A_{latm} = \begin{bmatrix} -4 & -600 & 0 & 0 \\ 0.1 & -10 & 0 & 0 \\ 0 & 0 & 0.6 & -1.1 \\ 0 & 0 & 2 & -2.2 \end{bmatrix}.$$

$$B_{lonm} = \begin{bmatrix} 0 & 0.5 \\ 0 & 0 \\ 10 & 0 \\ 0 & 0 \end{bmatrix} \quad B_{latm} = \begin{bmatrix} 0 & 0 \\ 10 & 0 \\ 0 & 0.5 \\ 0 & 0 \end{bmatrix}. \quad (43)$$
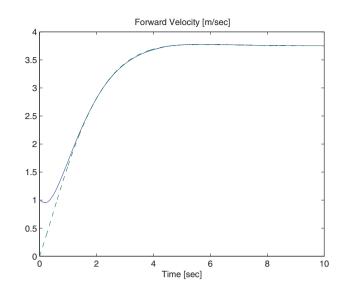
Figure 2. The reference velocity (dashed line) and the actual velocity (solid line).
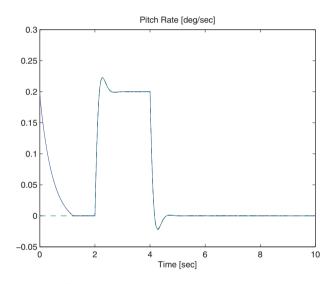
Figure 3. The reference pitch rate (dashed line) and the actual pitch rate (solid line).
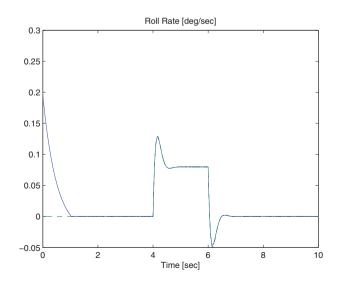
Figure 4. The reference roll rate (dashed line) and the actual roll rate (solid line).
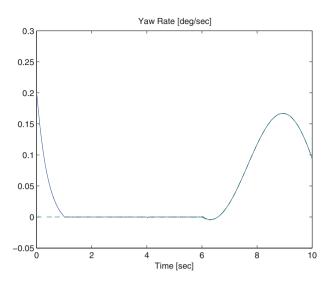
Figure 5. The reference yaw rate (dashed line) and the actual yaw rate (solid line).

Entries of the reference input $u_m(t) \in \mathbb{R}^4$ are elevator deflection angle, control thrust, aileron deflection angle and rudder deflection angle, respectively, and was designed as $u_m = [0.2\sin(t), 0.2, 0.2\sin(t), 0.2\sin(t)]^T$.
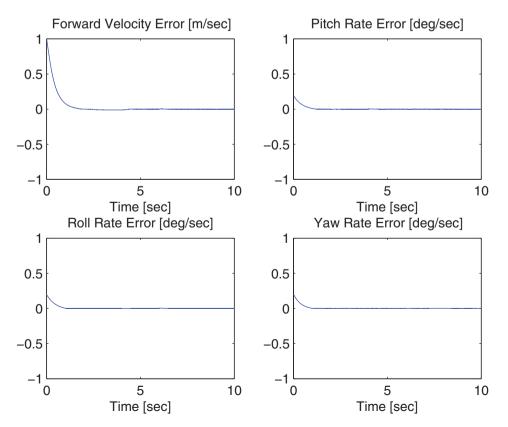
In order to obtain $Y(t)$, we began from the last (i.e. 4th) row of (9) and since, due to the structure of U, the last row of the term $(U - I_4)$ is zero, the fourth entry of $Y\phi$ is equal to the last entry of N_{LP} which has the form $N_{LP} = MCA\dot{x}_m - MCA_m\dot{x}_m - MCB_m\dot{u}_m$. Since the last entry of N_{LP} consists of reference model terms and uncertain constant parameters, it is easy to obtain

the linear parametrisation. Next, the third entry and then the other entries of the linear parametrisation can be found in a similar manner. Uncertain constant parameters are collected into a 300 by 1 vector. The details of the linear parametrisation including the complete structures of Y and ϕ can be found in Tanyer (2015).
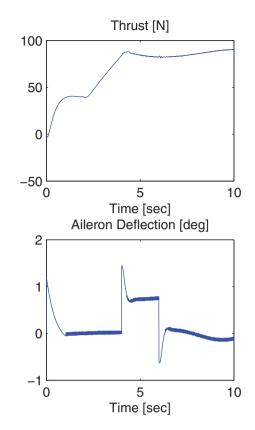
The control gains are required to satisfy the conditions given in Theorem 4.1. Adjusting these gains via trial-and-error is time-consuming and not easy. To ease this process, the self-tuning algorithms in Bidikli et al. (2013), Bidikli et al. (2014) designed for a similar class of nonlinear controllers were used as an add-on, and after the algorithm converged, numerical simulations were re-run for the final values of the control gains. Specifically, the final values of the control gains β and K were obtained from the self-tuning algorithm as

$$
\beta = \begin{bmatrix} 72.4 & 0 & 0 & 0 \\ 0 & 81 & 0 & 0 \\ 0 & 0 & 79.6 & 0 \\ 0 & 0 & 0 & 80.8 \end{bmatrix}
$$

$$
K = \begin{bmatrix} 300 & 0 & 0 & 0 \\ 0 & 300.03 & 0 & 0 \\ 0 & 0 & 300 & 0 \\ 0 & 0 & 0 & 300.1 \end{bmatrix} \tag{44}
$$

and Λ and adaptive gain matrix Γ in (13) were chosen as $2I_4$ and $2I_{300}$, respectively.

The tracking performance of the output states are given in Figures 2–5. The tracking error is presented in Figure 6 while the
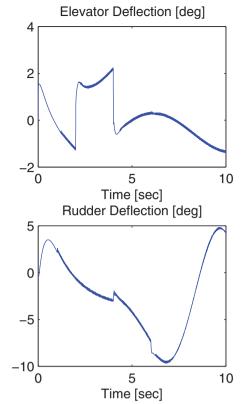

Figure 6. The output tracking error $e(t)$.

Figure 7. The control input $u(t)$.

Table 1. Tabulated steady-state error values for five simulation runs.

State	Average maximum steady-state error
Forward velocity	3.2×10^{-4}
Pitch rate	1×10^{-4}
Roll rate	3.6×10^{-3}
Yaw rate	1.6×10^{-3}

Table 2. Tabulated root mean square error values for five simulation runs.

State	Average root mean square error
Forward velocity	0.830
Pitch rate	0.088
Roll rate	0.086
Yaw rate	0.082

Table 3. Comparison of robust controller and robust adaptive controller.

Type of controller	K	β	Λ	Mean squared error
Robust	$100\,I_4$	$20\,I_4$	$2\,I_4$	7.1×10^{-2}
Robust adaptive	$100\,I_4$	$20\,I_4$	$2\,I_4$	5.6×10^{-2}
Robust adaptive	$100\,I_4$	$10\,I_4$	$2\,I_4$	6.1×10^{-2}
Robust adaptive	$100\,I_4$	$5\,I_4$	$2\,I_4$	6.4×10^{-2}
Robust adaptive	$100\,I_4$	$1\,I_4$	$2\,I_4$	6.8×10^{-2}

error is obtained with the adaptive controller even though the control gain β, which multiplies the integral of the sign of the error feedback term in (10), decreased significantly.

control inputs are given in Figure 7. From Figures 2–6, it is clear that the output tracking objective was satisfied. Specifically, from the stability analysis, $y \to y_m$ was proven, and from Figures 2–6, this convergence result can be observed to be achieved.

Five Monte–Carlo simulations were performed for different initial state values. In Tables 1 and 2, average maximum steady-state error and average root mean square error are presented, respectively. The steady-state error values in Table 1 show that the proposed controller ensures asymptotic tracking for different initial values of the states. In Table 3, a comparison of the robust adaptive controller and its non-adaptive version, obtained by setting $\hat{\phi}$ in (10) to zero, is given for different values of control gain matrices. From the first and last lines of Table 3, it is clear that approximately the same amount of mean squared

6. Conclusions

In this work, output tracking control of an aircraft that has parametric uncertainties in its state and input matrices was considered. The aircraft dynamics was considered to be under the influence of additive state- and/or time-dependent unstructured uncertainties as well. The control problem was further complicated by the availability of only the output measurements. To deal with these, a robust adaptive controller was designed. The controller was composed of three components where the first part was a proportional integral controller, the second part was an adaptive term, and the third part consisted of the integral of the sign of the error. The adaptive term was utilised to compensate for parametric uncertainties and the integral of the sign of the error feedback term was made use of to compensate for

unstructured uncertainties. Novel Lyapunov-type stability analysis techniques were utilised to ensure global asymptotic tracking of the output of a reference model. The performance of the proposed controller was demonstrated by comparative numerical simulations.

The main contributions of this study are now discussed. The uncertainties in the model of the aircraft are compensated under the restriction that only the output of the aircraft is available for the control design, and thus the need for acceleration measurements (such as in MacKunis, 2009; MacKunis et al., 2010) is removed. Acceleration measurements may be used in aircraft systems for system identification or control design. While acceleration measurements are available for some aircraft systems, utilising these measurements in control design may not be preferred from control theory perspective. Additionally, although accelerometers may be seen as good and practical solutions in system identification and control applications, there are several reasons for not using them in some applications. First, aside from onerousness in implementation, one needs to deal with sensor-related issues such as calibration and possible sensor failures. One way to avoid calibration requirements and sensor failures is, if possible, not to use them. For some cases, using them may be considered as redundant due to their costs. While the costs of sensors are decreasing rapidly, using them still adds to the cost of the overall system. Furthermore, aside from these, it should also be noted that using an additional sensor complicates the sensing system. The input gain matrix CB was not imposed symmetry or positive definiteness while compensating for the uncertainties in it. Furthermore, different from MacKunis (2009), the need for the estimation of the uncertain input gain matrix is removed. Finally, the four-step Lyapunov-based stability analysis that ensured global asymptotic stability is novel.

Notes

1. A preliminary version of this work was published in Tanyer et al. (2014).
2. Throughout the paper, I_n and $0_{m \times r}$ will be used to represent an $n \times n$ standard identity matrix and an $m \times r$ zero matrix, respectively.

Disclosure statement

No potential conflict of interest was reported by the authors.

References

Annamalai, A.S.K., Sutton, R., Yang, C., Culverhouse, P., & Sharma, S. (2015). Robust adaptive control of an uninhabited surface vehicle. *Journal of Intelligent & Robotic Systems, 78*(2), 319–338.

Arapostathis, A., George, R.K., & Ghosh, M.K. (2001). On the controllability of a class of nonlinear stochastic systems. *Systems & Control Letters, 44*(1), 25–34.

Bayrak, A., Tatlicioglu, E., Bidikli, B., & Zergeroglu, E. (2013). Robust adaptive control of nonlinear systems with unknown state delay. In *Asian control conference, Istanbul, Turkey* (pp. 1–6). New York, NY: IEEE.

Bidikli, B., Tatlicioglu, E., Bayrak, A., & Zergeroglu, E. (2013). A new Robust 'Integral of Sign of Error' feedback controller with adaptive compensation gain. In *International conference on decision and control, Florence, Italy* (pp. 3782–3787). New York, NY: IEEE.

Bidikli, B., Tatlicioglu, E., & Zergeroglu, E. (2014). A self tuning RISE controller formulation. In *American control conference, Portland, OR, USA* (pp. 5608–5613). New York, NY: IEEE.

Bidikli, B., Tatlicioglu, E., & Zergeroglu, E. (2015). Robust control of a rigid link in a cross flow. In *European control conference, Linz, Austria* (pp. 1231–1236). New York, NY: IEEE.

Bidikli, B., Tatlicioglu, E., Zergeroglu, E., & Bayrak, A. (2016). An asymptotically stable continuous robust controller for a class of uncertain MIMO nonlinear systems. *International Journal of Systems Science, 47*(12), 2913–2924.

Calise, A.J., & Rysdyk, R.T. (1998). Nonlinear adaptive flight control using neural networks. *IEEE Control Systems, 18*(6), 14–25.

Carrasco-Elizalde, A., & Goldsmith, P. (2015). Robust adaptive visual servoing of a robot. *International Journal of Robotics and Automation, 30*(4), 345–356.

Chen, J., Li, D., Jiang, X., & Sun, X. (2006). Adaptive feedback linearization control of a flexible spacecraft. In *International conference on intelligent systems design and applications* (pp. 225–230). Los Alamitos, CA: IEEE.

Costa, R.R., Hsu, L., Imai, A.K., & Kokotović, P. (2003). Lyapunov-based adaptive control of MIMO systems. *Automatica, 39*(7), 1251–1257.

Dawson, D.M., Hu, J., & Burg, T.C. (1998). *Nonlinear control of electric machinery*. New York, NY: Marcel Dekker.

Dixon, W.E., Behal, A., Dawson, D.M., & Nagarkatti, S. (2003). *Nonlinear control of engineering systems: A Lyapunov-based approach*. Boston, MA: Birkhauser.

Do, K.D. (2016). Global robust adaptive path-tracking control of underactuated ships under stochastic disturbances. *Ocean Engineering, 111*, 267–278.

Doman, D.B., & Ngo, A.D. (2002). Dynamic inversion-based adaptive/reconfigurable control of the X-33 on ascent. *Journal of Guidance, Control, and Dynamics, 25*(2), 275–284.

Dydek, Z., Annaswamy, A., & Lavretsky, E. (2010). Adaptive control and the NASA X–15–3 flight revisited. *IEEE Control Systems Magazine, 30*, 32–48.

Federal Aviation Administration (2002). *Federal aviation regulations: Airworthiness standards: Transport category airplanes*. Washington, WA.

Fei, J., & Zhou, J. (2012). Robust adaptive control of MEMS triaxial gyroscope using fuzzy compensator. *IEEE Transactions on Systems, Man, and Cybernetics, Part B: Cybernetics, 42*(6), 1599–1607.

How, J.P., Frazzoli, E., & Chowdhary, G. (2012). *Handbook of unmanned aerial vehicles, chapter nonlinear flight control techniques for unmanned aerial vehicles*. Netherlands: Springer.

Hussain, H.S., Annaswamy, A.M., & Lavretsky, E. (2016). *A new approach to robust adaptive control*. American control conference. Boston, MA.

Ioannou, P., & Sun, J. (1995). *Stable and robust adaptive control*. Englewood, NJ: Prentice Hall.

Jafari, S., & Ioannou, P.A. (2016). Robust adaptive attenuation of unknown periodic disturbances in uncertain multi-input multi-output systems. *Automatica, 70*, 32–42.

Khalil, H.K. (2002). *Nonlinear systems*. New York, NY: Prentice Hall.

Khooban, M.H., Niknam, T., Blaabjerg, F., Davari, P., & Dragicevic, T. (2016). A robust adaptive load frequency control for micro-grids. *ISA Transactions*. Advance online publication. doi:10.1016/j.isatra.2016.07.002

Krstic, M., Kanellakopoulos, I., & Kokotovic, P. (1995). *Nonlinear and adaptive control design*. New York, NY: John Wiley & Sons.

Lavretsky, E., & Hovakimyan, N. (2005). Adaptive compensation of control dependent modeling uncertainties using time-scale separation. In *IEEE conference on decision & control* (pp. 2230–2235). New York, NY: IEEE.

Liu, X.J., Lara-Rosano, F., & Chan, C. (2004). Model-reference adaptive control based on neurofuzzy networks. *IEEE Transaction on Systems, Man, and Cybernetics, Part C: Applications and Reviews, 34*(3), 302–309.

MacKunis, W. (2009). *Nonlinear control for systems containing input uncertainty via a Lyapunov-based approach* (Unpublished doctoral dissertation). University of Florida, Gainesville, FL.

MacKunis, W., Patre, P.M., Kaiser, M.K., & Dixon, W.E. (2010). Asymptotic tracking for aircraft via robust and adaptive dynamic inversion methods. *IEEE Transaction on Control Systems Technology, 18*(6), 1448–1456.

Mondal, S., & Mahanta, C. (2012). Adaptive second-order sliding mode controller for a twin rotor multi-input–multi-output system. *IET Control Theory & Applications, 6*(14), 2157–2167.

Stepanyan, V., & Kurdila, A. (2009). Asymptotic tracking of uncertain systems with continuous control using adaptive bounding. *IEEE Transaction on Neural Networks, 20*(8), 1320–1329.

Stevens, B.L., & Lewis, F.L. (2003). *Aircraft control and simulation*. New York, NY: John Wiley & Sons.

Tan, X., Su, X., Zhao, K., & Tan, M. (2015). *Robust adaptive backstepping control of micro-turbines*. Chinese control and decision conference. Yanchuan.

Tandale, M.D., & Valasek, J. (2005). Adaptive dynamic inversion control of a linear scalar plant with constrained control inputs. In *American control conference* (pp. 2064–2069). Portland, OR: IEEE.

Tanyer, I. (2015). *Development of nonlinear robust control techniques for unmanned aerial vehicles*. Izmir: Izmir Institute of Technology.

Tanyer, I., Tatlicioglu, E., & Zergeroglu, E. (2014). A robust adaptive tracking controller for an aircraft with uncertain dynamical terms. In *IFAC World Congress, Cape Town, South Africa* (pp. 3202–3207). Lazenburg: IFAC.

Tao, G. (2003). *Adaptive control design and analysis*. New York, NY: John Wiley & Sons.

Tatlicioglu, E. (2010). Adaptive control of teleoperator systems in the presence of additive input and output disturbances. *International Journal of Robotics and Automation, 25*(1), 17–25.

Wang, S., Li, J., & Wang, S. (2011). A dynamic inversion controller design for miniature unmanned aerial vehicles. In *International conference on consumer electronics, communications and networks* (pp. 1916–1921). New York, NY: IEEE.

Wise, K.A., Lavretsky, E., Gadient, R., & Ioannou, P.A. (2015). Robust, adaptive, and output feedback-based control systems – aircraft application and open challenges. In *American control conference, Chicago, IL, USA*. New York, NY: IEEE.

Xu, B. (2015). Robust adaptive neural control of flexible hypersonic flight vehicle with dead-zone input nonlinearity. *Nonlinear Dynamics, 80*(3), 1509–1520.

Yildiz, Y., & Annaswamy, A. (2015). Robust adaptive Posicast controller. In *IFAC workshop on time delay systems, Ann Arbor, Michigan, USA* (pp. 398–403). Laxenburg: IFAC.

Yu, L., & Fei, S. (2014). Robustly stable switching neural control of robotic manipulators using average dwell-time approach. *Transactions of the Institute of Measurement & Control, 36*(6), 789–796.

Yu, L., Fei, S., Sun, L., Huang, J., & Yang, G. (2014). Robustly stable switching neural control of robotic manipulators using average dwell-time approach. *International Journal of Computer Mathematics, 91*(5), 983–995.

Yu, L., Fei, S., Sun, L., Huang, J., & Yang, G. (2015). Design of robust adaptive neural switching controller for robotic manipulators with uncertainty and disturbances. *Journal of Intelligent & Robotic Systems, 77*(3), 571–581.

Yu, L., Fei, S., & Yang, G. (2015). A neural network approach for tracking control of uncertain switched nonlinear systems with unknown deadzone. *Circuits Systems & Signal Processing, 34*, 2695–2710.

Zhao, B., Xian, B., Zhang, Y., & Zhang, X. (2015). Nonlinear robust adaptive tracking control of a quadrotor UAV via immersion and invariance methodology. *IEEE Transaction on Industrial Electronics, 62*(5), 2891–2902.

Zou, Q., Wang, F., Zou, L., & Zong, Q. (2015). Robust adaptive constrained backstepping flight controller design for re-entry reusable launch vehicle under input constraint. *Advances in Mechanical Engineering, 7*(9). 1–13.

Zou, Y. (2016). Nonlinear robust adaptive hierarchical sliding mode control approach for quadrotors. *International Journal of Robust and Nonlinear Control*. Advance online publication. doi:10.1002/rnc.3607